JOURNAL OF MATERIALS SCIENCE 32 (1997) 3705–3710

Electrical and morphological characterization of a nickel–polyester composite prepared by spreading and spraying techniques

M. M. DÁVILA, M. P. ELIZALDE, R. SILVA
(1) Facultad de Ciencias Químicas; (2) Centro de Química; (3) Instituto de Física, Universidad Autónoma de Puebla, Apdo. Postal No J-55, Puebla, Pue. 72571, Mexico

Nickel–Polyester samples were produced using polyester resin and metallic particles of nickel. A scanning electron microscopy study shows that the prepared surface produced from nickel particles dispersed in the polyester and thermally treated consists of a porous network. Nickel–Polyester composites with resistivity values around 10^{-1}–10^{-3} Ω cm have been analysed as potential oxygen evolution electrodes in an alkaline medium. The dependence of the electronic parameters on the morphological features of the nickel–polyester samples is evident from the study carried out with samples prepared at different conditions.

1. Introduction

In recent decades an extensive research effort has been directed towards the production of composite materials such as granular metal films [1], conductor insulator composites [2], cast composites [3], and disordered semiconductors [4]. Composites are used in the automotive industry and as energy conversion devices [5, 6], as antistatic products, electromagnetic interference (EMI) and radio frequency interference (RFI) shielding materials [7–10]. Composite materials can be adjusted to satisfy different requirements by using different procedures [11–15]. The electrical and physical properties of polymer composites containing fine particles (e.g., metal and ceramic powders, chopped carbon fibres, charge transfer salts, etc.) in random and segregated distributions have been investigated by several groups [13, 14, 16–21]. These properties can be affected by the concentration of the conductive filler, the particle structure, its size and shape, the state of aggregation and agglomeration, the size distribution, matrix morphology, mixing efficiency, temperature and also the application of an alternating electric or magnetic field during polymerization of the composite. Conductive composites can be obtained by compaction of a mixture of powders comprising a polymeric insulator (polyethylene, polyvinyl chloride, polycarbonate) and a metallic conductor (nickel, copper, silver, iron) or by mixing the components in a plastograph at different temperatures and subsequent moulding. In the present paper, we report investigations of the influence of the method of preparation on the morphology and the conductive and electrochemical behaviour for a series of nickel–polyester samples.

2. Experimental procedure

2.1. Preparation of the nickel polyester composite

The nickel–polyester samples were prepared using the polyester resin Escil Sody 33 and Sody 33C as a catalyst, into which the weighed portions of nickel powder 99.99% Merck (with a particle size $< 10\,\mu m$) were dispersed by milling. Acetone or methyl ethyl ketone were used as a solvent [22]. Plaques of nickel–polyester composite were prepared by two procedures. In the first case the mixtures were spread over a glass surface with drawbars. In the second method the nickel–polyester resin suspension was sprayed onto a pyrex glass substrate held at room temperature employing air as the carrier gas [22]. After air drying, the composite samples were cured for 36 h at room temperature or 1 h under vacuum (1.333×10^{-3} Pa). Afterwards they were treated at selected temperatures between 50–170 °C in air for different time periods [22] after which they were removed from the glass substrate. The thickness of the samples, determined by scanning electron microscopy (SEM), was around 70–100 μm for the samples prepared by spraying the nickel–polyester resin and 300–400 μm for plaques obtained with the drawbars. Porosity measurements were carried out on the nickel powder and also on samples of the Ni-polyester composites. A glass container of known volume and weight was filled with nickel powder or plaques of the Ni-polyester composites and distilled water. The volume of liquid inside the sample was determined from the weight of distilled water able to find a place between nickel particles packed in the glass container. The porosity was established by weighing dry samples and samples soaked with water, a technique discussed in reference [23].

0022–2461

2.2. Morphology and electrical conductivity

The morphological characteristics of the nickel–polyester composite samples were determined using a JSM 5400 LV scanning electron microscope. The specimens for SEM examination were prepared by the commonly used procedure but without any evaporated film coating. The resistivity measurements were obtained by the van der Pauw technique [24] using a Keithley 195-A digital multimeter with an error of $\pm 0.02\%$ in conjunction with a 224 programmable current source (error $\pm 0.1\%$; stability $\pm 0.05\%$) and also by the four-point method. In all resistivity measurements plaques with an approximate 100 or 400 μm thickness were used. The contacts onto the samples were made with metallic silver wires (1 mm diameter) and metallic silver paint (Demetron).

2.3. Electrochemical measurements

For the electrochemical and electrical studies, contact between the nickel–polyester composite surface and the copper wire was made with the help of a clamp. Only a 0.4×0.4 cm surface area of the nickel–polyester composite was used for the study and the rest was isolated with epoxy resin. All the electrochemical experiments were performed in a three-compartment glass cell at room temperature. The electrolyte solution was prepared with KOH (Merk) and deionized water, and deaerated with nitrogen. The potential of the working electrode (nickel–polyester) was measured against a Hg/HgO reference electrode in the same solution, via a Luggin capillary. The counter electrode was a platinum foil. The electrochemical measurements were made using a potentiostat-galvanostat. The electrochemical behaviour of the nickel–polyester composite electrodes was determined using both the potentiodynamic and also the steady-state potentiostatic method.

3. Results and discussion

3.1. Morphology and electrical conductivity

Scanning electron microscope studies have indicated that the nickel particle surface morphology was highly spiky and angular (Fig. 1) while the superficial morphology of the nickel–polyester samples prepared at room temperature using drawbars consists of nickel particle aggregates embedded in polyester resin (Fig. 2). When the samples are prepared by spraying the nickel powder–polyester mixture onto a pyrex glass substrate held at room temperature the SEM micrographs show that the surface of the nickel–polyester composite is more porous (Fig. 3) and has less polyester resin between aggregates of nickel particles. This was confirmed by the values of porosity α for the nickel-polyester plaques obtained with drawbars ($\alpha = 0.36$) and for the nickel–polyester samples prepared by spraying ($\alpha = 0.61$). The porosity α of nickel powder was 0.5. When the samples were heat treated up to 150 °C, the plaques contained holes and showed a low mechanical strength (Fig. 4). The surface of these samples exhibits a porous network, and has a uniform

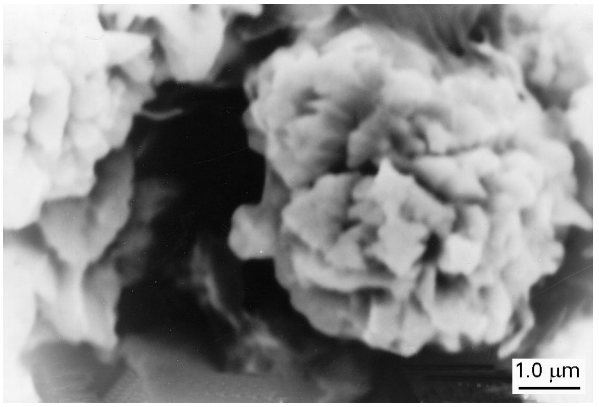

Figure 1 Morphology of the nickel metallic particles.

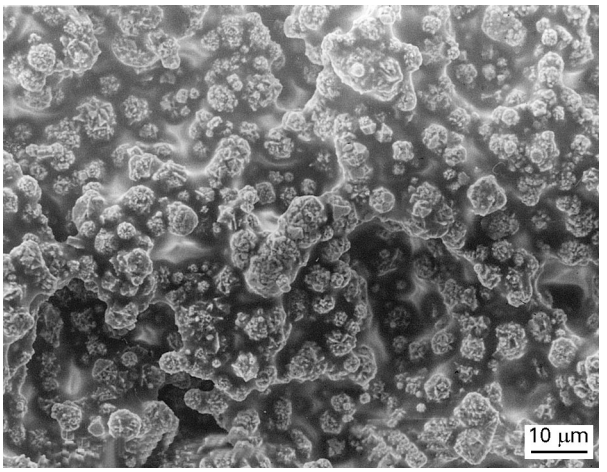

Figure 2 Superficial morphology of the nickel–polyester sample prepared using drawbars and curing at room temperature for 36 h.

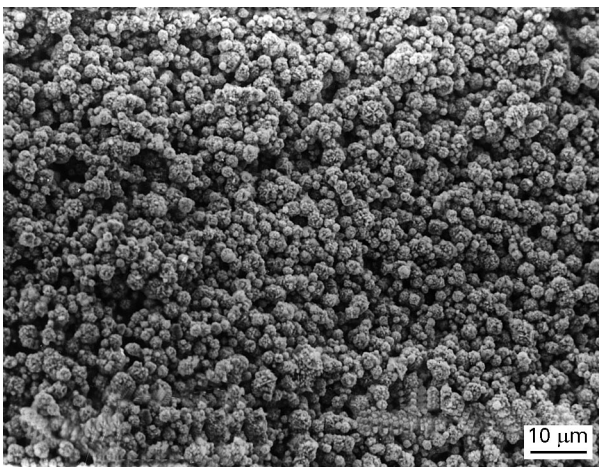

Figure 3 SEM micrograph of the nickel–polyester composite prepared by spraying the nickel powder–polyester mixture and curing without thermal treatment.

distribution of nickel in the bulk plaque. Scanning electron microscopy studies showed that the heat treatment of samples of nickel–polyester 1 h after preparation, induces the polymer to flow out from the aggregate (Fig. 5), producing a decrease of the insulating barrier and the formation of holes (Fig. 6) and at the same time an increase in the contact between adjacent particles or aggregates (Fig. 7). It should be

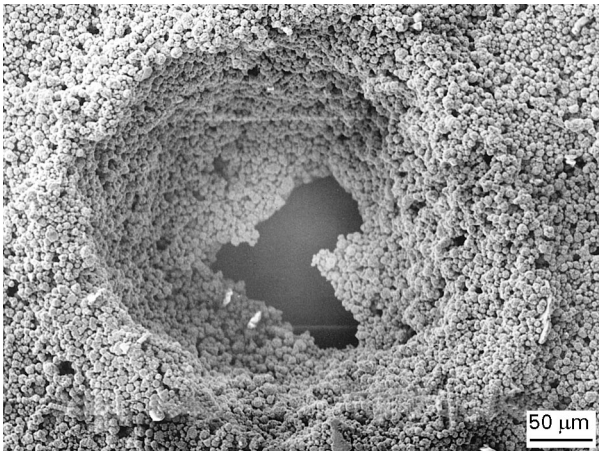

Figure 4 Structure of the bulk for a nickel–polyester sample (prepared using drawbars) after thermal treatment (around 150 °C) by SEM

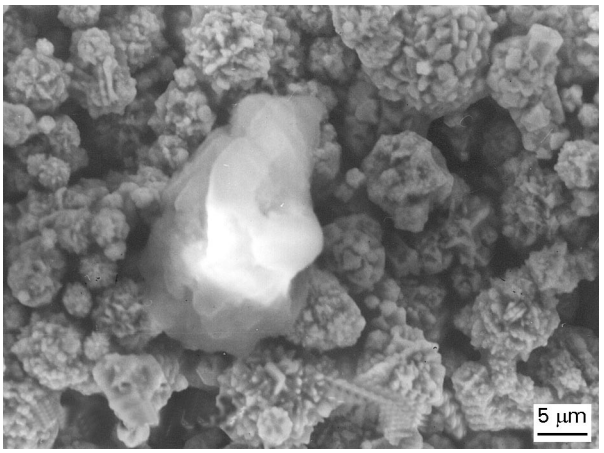

Figure 5 SEM micrograph of a nickel–polyester composite surface showing polymer flow between the aggregates.

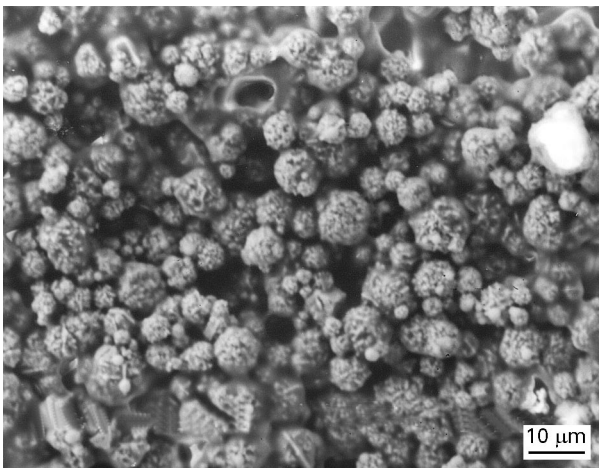

Figure 6 Formation of holes and pores on the surface of the nickel–polyester composite prepared using drawbars after thermal treatment.

noted that Figs 5 and 6 were obtained by a short heat treatment followed by a quick cooling of the plaques. Thermal shock favoured the solidification of the following resin. Since curing of the resin in the composite obtained by procedure [22] is completed in more than

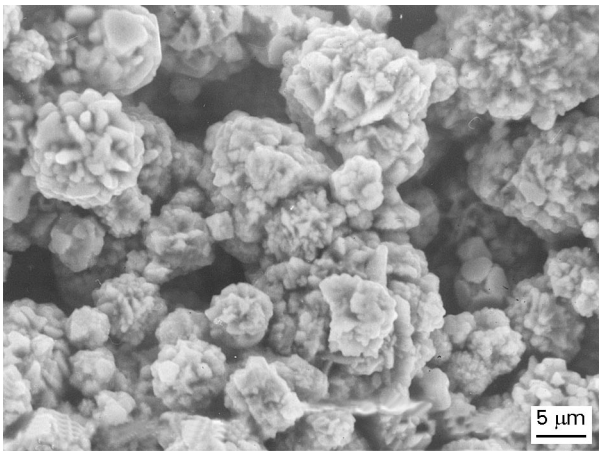

Figure 7 SEM micrograph of micron-sized aggregates of nickel–polyester composite. After Davila [22].

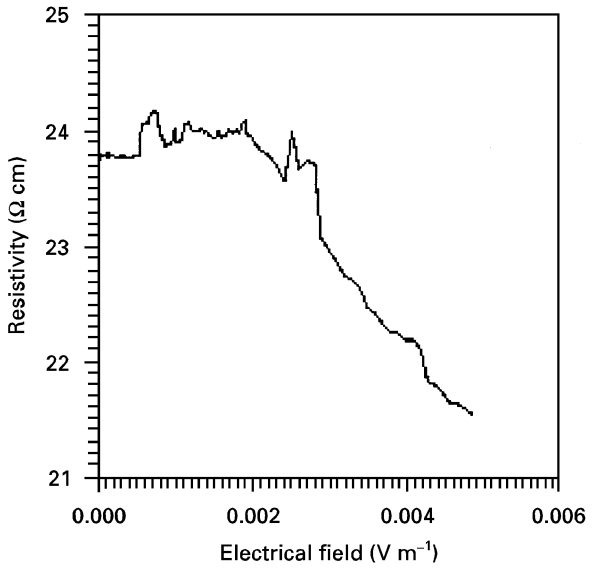

Figure 8 Resistance fluctuation of a nickel–polyester sample prepared using drawbars without thermal treatment.

36 h, the surface is covered by a low cross-linked resin. The thermal treatment accelerates the curing process yielding a nickel network composed finally of micron sized aggregates of nickel composites (Fig. 7) for samples obtained with both drawbars and for plaques prepared by spraying. However, thinner and more homogeneous plaques can be obtained using the spray method. We observed that the heat treatment yields composites with a higher porosity. This fact can be explained by the formation of microholes and partial evaporation of the resin leaving bare nickel particles (compare Figs 1 and 7) on the surface.

The dependence of the electrical properties on the morphological features of the nickel–polyester composite samples is evident from the study carried out with samples prepared at different temperatures and by two different methods. The resistivity value was of the order of 10^{-3} and 10^{-2} Ω cm for both samples after the thermal treatment. In the case of samples prepared using drawbars and cured at room temperature i.e., without thermal treatment, they showed fluctuations or resistance drift (Fig. 8), which might be

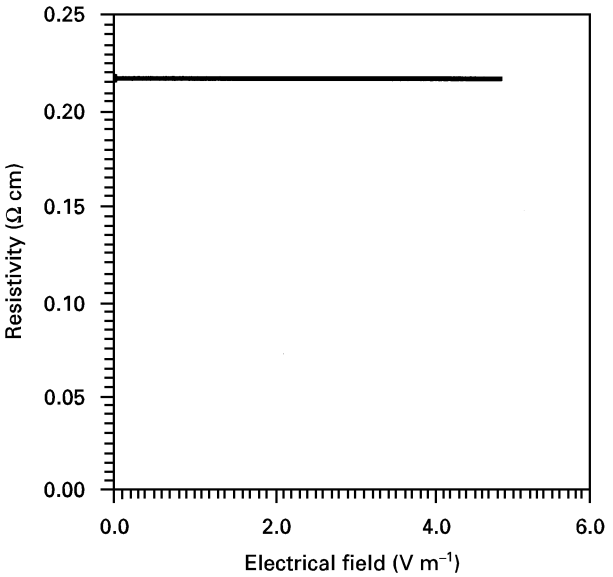

Figure 9 Resistivity of a nickel–polyester sample obtained by drawbars at room temperature after the thermal treatment.

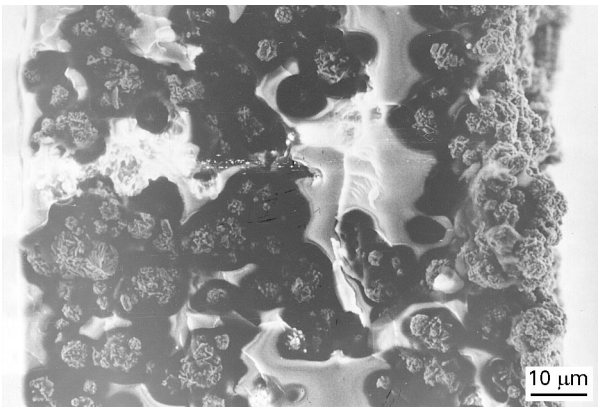

Figure 10 Cross-section of a nickel–polyester plaque prepared by the spraying technique.

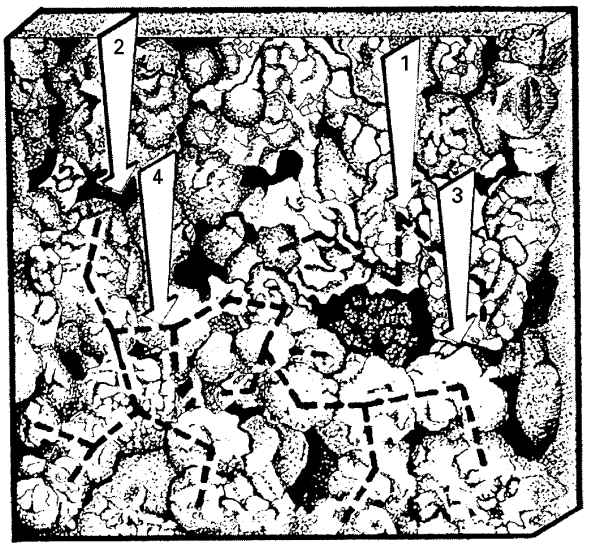

Figure 11 Sketch of the aggregate-to-aggregate conduction in a polyester medium. (1) Aggregates of nickel covered with insulating polyester film, (2) insulating medium, (3) interstitial spaces, (4) conducting paths.

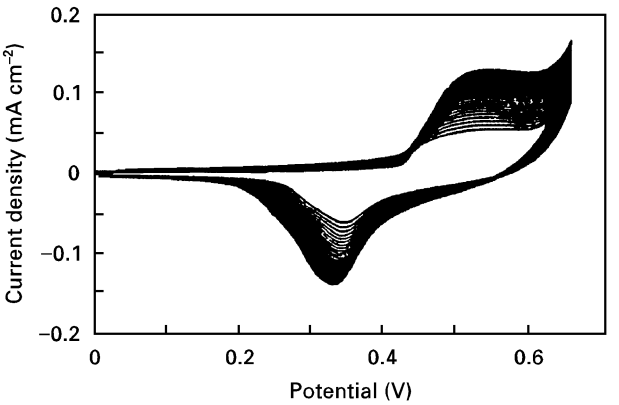

Figure 12 Voltammetric behaviour of the nickel–polyester electrode prepared using drawbars in 1 M KOH with continuous potential cycling (20 cycles); at $x = 30\ \mathrm{mV\,s^{-1}}$.

the effect of the insulating barrier thickness or destructive effects due to Joule heating during the measurements. When the nickel–polyester samples prepared but not fully cured are heat treated (50–120 °C), the resistivity is two orders of magnitude less (Fig. 9) than those prepared without thermal treatment. This suggests that the cause of the resistivity change is the insulating polymer layer between the nickel aggregates (see Figs 2 and 3). The cross-section of the nickel–polyester samples, shown in Fig. 10 indicates a random dispersion of the nickel particles in the bulk.

The current–voltage characteristics of all these samples were ohmic in the low field measurement region. At high electrical fields (70–90 V m^{-1}) resistance drifts due to Joule heating were observed. The Joule heating during the measurements at high fields can lead to an alteration of the microstructure and conduction pathway. This can explain the fact that returning to low fields and repeating measurements starting from low to high fields, the resistivity values reach $1 \times 10^{-1}\ \Omega$ cm. The contribution made to the resistivity by changes in the network due to Joule heating is around one order of magnitude. On the basis of previous publications [25, 26], we consider that the electrical conductivity of the nickel–polyester results from electron tunnelling across the small barriers that separate the conductive pathways (Fig. 11). The conductivity is however controlled by the shape of the tunnelling barrier, the larger the insulating barrier, the lower the conductivity and the higher the apparent energy barrier. This can explain both the effect of the preparation temperature and the morphology of the nickel–polyester samples.

3.2. Electrochemical characterization

The combination of a good mechanical strength and good electrical properties for the nickel–polyester composite enable it to be used as an electrode. Since electrodes have to sustain high electric currents, their electrical properties are considered to be of significant importance for their performance. The voltammetric response of nickel–polyester electrodes that did not undergo a thermal treatment in alkaline solution shows a very broad oxidation peak and a small current density (Fig. 12) while potentiodynamic curves

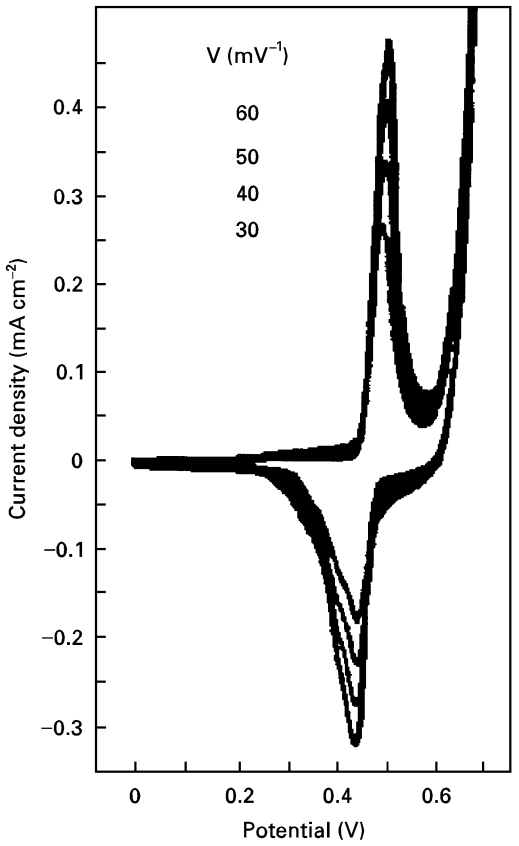

Figure 13 Cyclic voltammograms in 1 M KOH for a nickel–polyester electrode after thermal treatment.

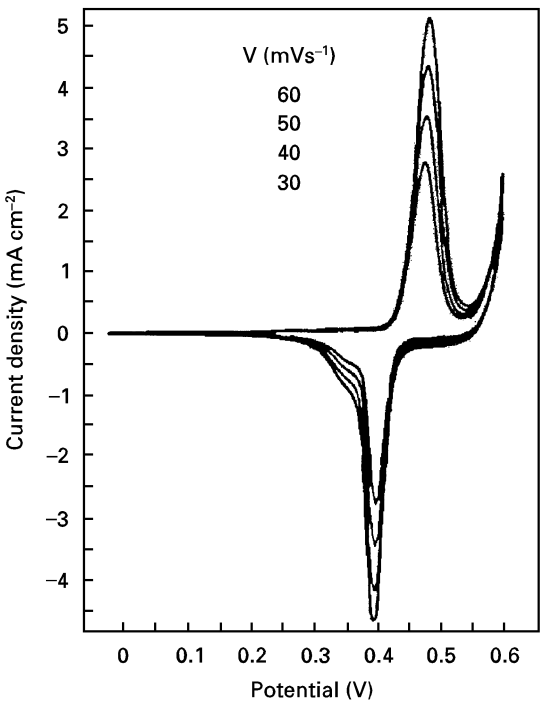

Figure 14 Voltammetric behaviour of the nickel foil electrode in 1 M KOH.

obtained for the nickel–polyester composite (Fig. 13) and massive nickel foil (Fig. 14) in 1M KOH show an oxidation peak related to the formation of nickel oxyhydroxide in its various phases [27]

$$\begin{array}{ccc} \alpha\text{-Ni(OH)}_2 & \leftrightarrow & \gamma\text{-NiOOH} + \text{H}^+ + \text{e}^- \quad (1) \\ \updownarrow & & \updownarrow \\ \beta\text{-Ni(OH)}_2 & \leftrightarrow & \beta\text{-NiOOH} + \text{H}^+ + \text{e}^- \quad (2) \end{array}$$

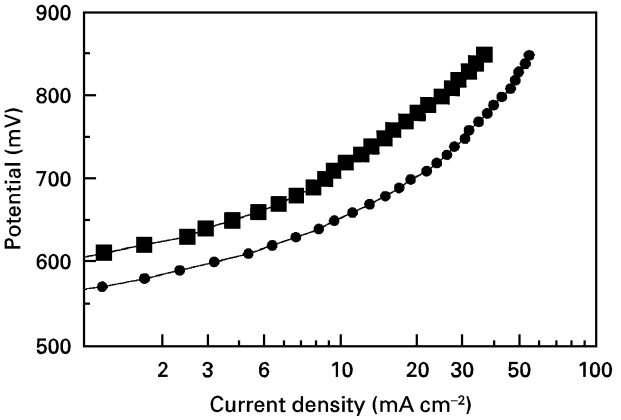

Figure 15 Apparent Tafel plots for oxygen evolution reaction in 3 M KOH on a nickel electrode: (●) nickel foil, (■) nickel–polyester.

The peak height and its area are greater for the nickel foil in comparison with the nickel–polyester composite. This behaviour is in agreement with the variation in the morphology and the electrode–solution interfacial area. The morphological differences between the nickel–polyester composite and the nickel foil electrodes leads to a variation in the efficiency of the electrode towards the oxygen evolution reaction (Fig. 15). The existence of insulating films of polyester around the aggregates of nickel particles decreases the active electrode surface, leaving only a reduced amount of nickel sites exposed to the electrolyte. This fact can explain the point that although one could expect a high efficiency in the oxygen evolution and charge–discharge values for the porous nickel–polyester surface, it in fact does not occur. However the nickel–polyester surface electrodes showed good stability and reproducibility (Table I). The results presented in this table show, that the apparent current density of the electrode at steady-state potentials was stable at low potentials (0.6–0.7 V) after staying in an air atmosphere. However the apparent current density is higher at very positive potentials (0.75–0.90 V). It is possible that at high positive potentials, species with high catalytic properties are present on the electrode. The obtained exchange current density i_0 of approximately 10^{-8} mA cm^{-2} and the results obtained in the present work for the Tafel slope in the low overpotential region studied under steady-state potentiostatic conditions in alkaline solutions are similar to values previously reported in the literature [28]. A recent study in our laboratory has shown that the charge–discharge capacity and oxygen evolution reaction efficiency can be increased, by the application of different surface treatments.

4. Conclusions

The results obtained show a clear effect of the method of preparation and treatment of the Ni–polyester composites on the morphology, resistivity and on the electrocatalytic activity for the oxygen evolution reaction in alkaline solutions. A layer of insulating polymer is maintained between touching aggregates which is the reason for the coexistence of a tunnelling

TABLE I Kinetic parameters for the oxygen evolution reaction of the nickel–polyester electrode in x M KOH at 25 °C

Electrode pretreatment	Concentration KOH (mol dm^{-3})	Apparent current density i, (mA cm^{-2})					
		600 mV	700 mV	800 mV	900 mV	b (mV dec^{-1})	i_0 ($\times 10^{-8}$ mA cm^{-2})
Fresh electrode	1.0	0.94	13.5	35.0	58.0	60	1.6
After 21 h	1.0	0.96	15.0	44.0	72.0	60	1.2
Fresh electrode	2.0	3.0	23.0	55.0	94.0	55	2.4
After 14 h	2.0	2.9	29.0	72.0	115.0	55	2.0
Fresh electrode	5.0	11.0	48.0	105.0	175.0	55	6.8
Aged electrode[a]	5.0	15.0	64.0	125.0	200.0	55	5.1

The Tafel slope (b) and the exchange current densities (i_0) for the oxygen evolution reaction are obtained from the oxygen overpotentials and the logarithm of current density plots (Tafel equation)

[a] This type was obtained by subjecting the freshly prepared electrodes to potentiodynamic cycles at 0.03 Vs^{-1} in the potential region were the oxygen evolution reaction takes place.

conductance and a percolation like network in the nickel–polyester composite. The mechanical strength and electrical properties of the nickel–polyester composites are retained after chemical or electrochemical treatment in alkaline electrolytes, therefore they can be used in electrocatalysis and other fields.

Acknowledgements

This work was supported by Consejo Nacional de Ciencia y Tecnología (Project 3297-E). The authors are grateful to Dr Francisco Silva for valuable discussions.

References

1. P. SHENG, B. ABELES and Y. ARIE, *Phys. Rev. Lett.* **31** (1973) 44.
2. J. DRESNER, K. W. HANG, J. I. GITTLEMAN and P. KUZNETSOFF, *J. Non-Cryst. Solids* **27** (1978) 39.
3. S. RAY, *J. Mater. Sci.* **28** (1993) 5397.
4. D. REDFIELD, *Phys. Rev. Lett.* **30** (1973) 1319.
5. C. IWAKURA, N. FURUKAWA and M. TANAKA, *Electrochim. Acta* **37** (1992) 759.
6. M. K. CARPENTER, R. S. CONELL and D. A. CORRIGAN, *Solar Energy Mat.* **16** (1987) 333.
7. Y. KUMAGAI, K. URABE and T. KANBE, *J. Jpn. Soc. Compos. Mat* **11** (1985) 15.
8. S. NAIK, M. CORNEL and M. FENTON, in Proceeding of the 41st Annual Conference of the Reinforced Plastics/Composites Institute January 1986. (The Society of Plastics Industry 1986) *Rev. Plast. Mod.* **51** (1986) 457.
9. J. M. CROSBY and J. E. TRAVIS, *Rubber World* **193** (1985) 30.
10. M. T. KORTSCHOT and R. T. WOODHAMS, *Polym. Compos.* **6** (1985) 296.
11. A. K. GARG and L. C. DEJANGHE, *J. Mater. Sci.* **28** (1993) 3427.
12. B. JACHYM, I. WITORT and G. WISNIEWSKI, *Synthetic Metals* **29** (1989) F259.
13. A. MALLIARIS and D. T. TURNER, *J. Appl. Phys.* **42** (1971) 614.
14. D. DAS, S. BASU and A. PAUL, *J. Mater. Sci* **15** (1980) 1719.
15. S. JIN, T. H. TIEFEL and R. WOLFE, *IEEE Trans, Magn.* **28** (1992) 2211.
16. J. GURLAND. *Trans. Metal. Soc. AIME* **236** (1966) 642.
17. R. P. KUSY and D. T. TURNER, *Nat. Phys. Sci* **229** (1971) 58.
18. R. P. KUSY, *J. Appl. Phys.* **48** (1977) 530.
19. D. M. BIGG, *Polym. Engng. Sci.* **19** (1979) 1188.
20. S. K. BHATTACHARYA, S. K. DE and S. BASU, *Polym. Engng. Sci* **19** (1979) 21.
21. S. K. BHATTACHARYA, S. K. DE and A. C. D. CHAKLADER, *Polymer. Plast. Tech. Engng.* **19** (1982) 21.
22. M. M. DAVILA, Mexican Patent BUAP 05171 (1994)
23. J. P. CANDY, P. FOUILLOUX, M. KEDDAM and H. TAKENOUTI, *Electochim. Acta* **26** (1981) 1029.
24. L. J. VAN DER PAUW, *Philips Res. Rep* **13** (1958) 1.
25. Y. BALBERG, *Phys. Rev. Lett.* **59** (1987) 1305.
26. P. SHENG, *Phys. Rev.* **B21** (1980) 2180.
27. H. BODE, K. DEHMELT and J. WITTE, *Electrochim. Acta* **11** (1966) 1079.
28. P. W. J. LU and S. SRINIVAN, *J. Electrochem. Soc.* **125** (1978) 1416.

Received 25 March
and accepted 19 December 1996